European Heart Journal Cardiovascular Imaging (2012) **13**, 730–738
doi:10.1093/ehjci/jes026

Correlates of global area strain in native hypertensive patients: a three-dimensional speckle-tracking echocardiography study

Maurizio Galderisi*, Roberta Esposito, Vincenzo Schiano-Lomoriello, Alessandro Santoro, Renato Ippolito, Pierluigi Schiattarella, Pasquale Strazzullo, and Giovanni de Simone

Echocardiography Laboratory, Cardioangiology with CCU, Department of Clinical and Experimental Medicine, Federico II University Hospital, Block 1, Via S. Pansini 5, 80131 Naples, Italy

Received 27 September 2011; accepted after revision 11 January 2012; online publish-ahead-of-print 9 February 2012

Aims The present study aimed to test the capability of real-time three-dimensional echocardiography (RT3DE) in characterizing early abnormalities of left ventricular (LV) structure and function in native, untreated hypertensive patients.

Methods and results Thirty-eight newly diagnosed, never-treated hypertensives (H) and 38 healthy controls (C) underwent both standard echo-Doppler and RT3DE assessment. LV volumes and ejection fraction (EF), sphericity index, LV mass index (LVMi), global longitudinal strain (GLS), global circumferential strain (GCS), global area strain (GAS), and global radial strain (GRS) were calculated by RT3DE. The two groups were comparable for age and heart rate. Body mass index and blood pressure (BP) were significantly higher in H. LV volumes, EF, and sphericity index calculated by RT3DE did not differ significantly between the two groups, while LVMi was higher in H than in C ($P < 0.0001$). GAS ($-29.1 \pm 2.5\%$ in H vs. $-33.6 \pm 3.4\%$ in C), GLS, and GRS (all $P < 0.0001$) were lower in H, but GCS was not significantly different between the two groups. Among the different 3D strain components, GAS showed the best independent associations with mean BP ($\beta = -0.502$, $P < 0.0001$) and LVMi ($\beta = -0.385$, $P < 0.001$; cumulative $R^2 = 0.55$, $P < 0.0001$) in the pooled population.

Conclusion RT3DE identifies early functional LV changes in native hypertensive patients. GAS is precociously reduced, and longitudinal and radial strain impaired, while circumferential strain is still preserved, supporting a normal LV chamber systolic function. Reduction of GAS is independently associated with both pressure overload and magnitude of the LV mass.

Keywords Real-time three-dimensional echocardiography • Speckle-tracking echocardiography • Global longitudinal strain • Area strain • Arterial hypertension

Introduction

The heart involvement in arterial hypertension is currently evaluated by standard echocardiography. Measurements of left ventricular (LV) mass identify LV hypertrophy, whereas relative wall thickness categorizes LV concentric or eccentric (normal) geometry.[1] LV hypertrophy is an independent predictor of morbidity and mortality[2] and LV mass reduction induced by antihypertensive therapy improves the prognosis.[3,4] The importance of LV functional assessment in hypertensive heart disease by traditional methods is more debated. However, the majority of studies in hypertensive cohorts uses measures of LV systolic function derived from standard 2D echocardiography and Doppler indices of LV diastolic function.[5,6]

An innovative evaluation of LV function has recently become available by two-dimensional (2D) speckle tracking echocardiography (STE), a non-Doppler technique that allows to quantify myocardial deformation in the different spatial directions.[7] By

* Corresponding author: Tel: +39 81 7464749; Fax: +39 81 5466152, Email: mgalderi@unina.it

this technique, longitudinal strain has been demonstrated to be the first component of systolic deformation to be modified in native hypertensive patients when the LV geometry is still normal but diastolic abnormalities are already detectable.[8] Longitudinal strain is lower in hypertensive patients with than in those without LV hypertrophy.[9] Impaired longitudinal strain is associated with serum tissue inhibitor of matrix metalloproteinase, which suggests that a change in collagen turnover and the myocardial fibrotic process may take place in this early LV dysfunction.[10]

Further technological advancement of real-time three-dimensional echocardiography (RT3DE) has developed software that tracks the motion of speckles irrespective of their direction and allows to obtain a homogeneous spatial distribution of all three components of the myocardial displacement vector.[7] The main advantage of 3D STE is the possibility of analysing the whole left ventricle from a single volume of data obtained from the apical transducer position. In addition, its use considerably reduces the time duration of analysis to one-third in comparison with 2D STE.[11] 3D STE has been already used in patients with and without heart disease[12] and to assess LV mechanical dyssynchrony.[13] There is no information on the applicability of 3D STE to detect early LV systolic dysfunction in the context of untreated arterial hypertension. Accordingly, we evaluated whether 3D STE can be used to assess early LV systolic dysfunction before impairment of traditional indices of LV chamber function in native hypertensive patients, by identification of all the spatial components of myocardial deformation. We used RT3DE assessment including estimation of LV ejection fraction (EF) and shape, LV mass, and STE deformation parameters as an alternative to standard echocardiography.

Methods

Study population

The study population included new consecutive, young outpatients with uncomplicated arterial hypertension referring to the European Society of Hypertension (ESH) Excellence Center of Clinical and Experimental Medicine Department, Federico II University Hospital, from September 2010 to September 2011, and young healthy controls recruited from the personnel of our University staff and their relatives within a screening programme for primary cardiovascular prevention.

Arterial hypertension was defined according to the current ESH—European Society of Cardiology recommendations.[14] To be eligible, patients had to be newly diagnosed, never treated, and $\leq$45 years old (the latter criterion adopted also for healthy controls). Subjects were excluded from the study if they had poor echo quality (inadequate 3D full-volume acquisition or analysis). Eighty-four subjects were initially evaluated. After exclusions (five hypertensive patients and three healthy controls), the study population consisted of 38 hypertensive patients and 38 healthy controls. All the participants gave their written informed consent.

Procedures

Standard echo-Doppler examinations were performed using a 2.5 transducer with harmonic capability and RT3DE data set acquisition of the left ventricle obtained using a 3D volumetric transducer of a Vivid E9 ultrasound machine (GE Healthcare, Horten, Norway). At the end of echocardiographic examination, heart rate (HR) and blood pressure (BP) (average of three measurements by a cuff sphygmomanometer) were recorded.

Standard echo-Doppler examination

2D and Doppler standards of our laboratory have been previously described.[15] The quantitative analysis of the left ventricle was performed as recommended.[1] 2D LV EF was derived from LV end-diastolic and end-systolic volumes (average of the measurements in apical four- and two-chamber views) calculated according to the modified Simpson rule. LV mass was calculated by 2D-guided M-mode imaging using the Devereux and Reichek formula and indexed for height powered to 2.7. Left atrial volume (area-length method, average of measurements in apical four- and two-chamber views) was indexed for body surface area.[1] Transmitral Doppler inflow and tissue pulsed Doppler were recorded in the apical four-chamber view. The average of the peak early diastolic relaxation velocity (e′) of the septal and lateral mitral annulus was computed and the ratio of the transmitral peak early velocity (*E*) to average e′ (*E*/e′ ratio) calculated as a reliable estimate of invasively determined LV filling pressure.[16]

Real-time 3D echocardiography

A full-volume scan was acquired by harmonic imaging from an apical approach, using a frame rate (in volume per second) higher than 40% of the individual heart beat in order to increase the possibility that the 'speckles' could be recognizable in successive frames. Accordingly, four electrocardiogram-gated consecutive beats were acquired during end-expiratory apnoea (multi-beat acquisition) to generate the full volume from single-beat sub-volumes. The quality of acquisition was verified in each patient, before storing the volume data set, by selecting a 12-slice display mode available on the machine to ensure the entire LV cavity and wall were included in the full volume (*Figure 1*). When the acquisition was considered suboptimal, the data set was re-acquired.

Data sets were stored digitally in raw data format and exported to a separate workstation (Echopac, PC 110.1.1, GE Healthcare) equipped with a commercially available software (4D Auto LVQ software, GE Healthcare) for off-line analysis of LV volumes, EF, LV mass, and 3D STE deformation parameters. LV analysis was performed according to a previously described methodology.[17] It included the following steps:

(i) automatic slicing of the full LV volume data set;
(ii) alignment by pivoting and translating the four-chamber plane (aligning one plane automatically changes the other);
(iii) automated identification of the endocardial border both at end-diastole (LV end-diastolic volume) and end-systole (LV end-systolic volume) with manual adjustment of endocardial borders when the automated tracing was considered insufficient (manually corrected AutoLVQ);
(iv) final quantitative analysis and data display.

By the reported approach, the sphericity index [ratio between the measured LV end-diastolic volume and the theoretical spherical volume obtained from the end-diastolic long-axis dimension (LAD) as $4/3 \times \pi \times \frac{1}{2}$ LAD], and LV end-diastolic (EDV, mL) and LV end-systolic volume (ESV, mL) were calculated and the stroke volume (SV, mL = EDV − ESV), cardiac output (CO, L/m = SV × HR), and EF [% = (EDV/ESV)/EDV × 100] were derived (*Figure 2*).

In addition, recent developments of the software were applied to calculate the LV mass and strain .[18] LV mass [(LV epicardial volume − LV endocardial volume) × 1.05] was estimated at end-diastole

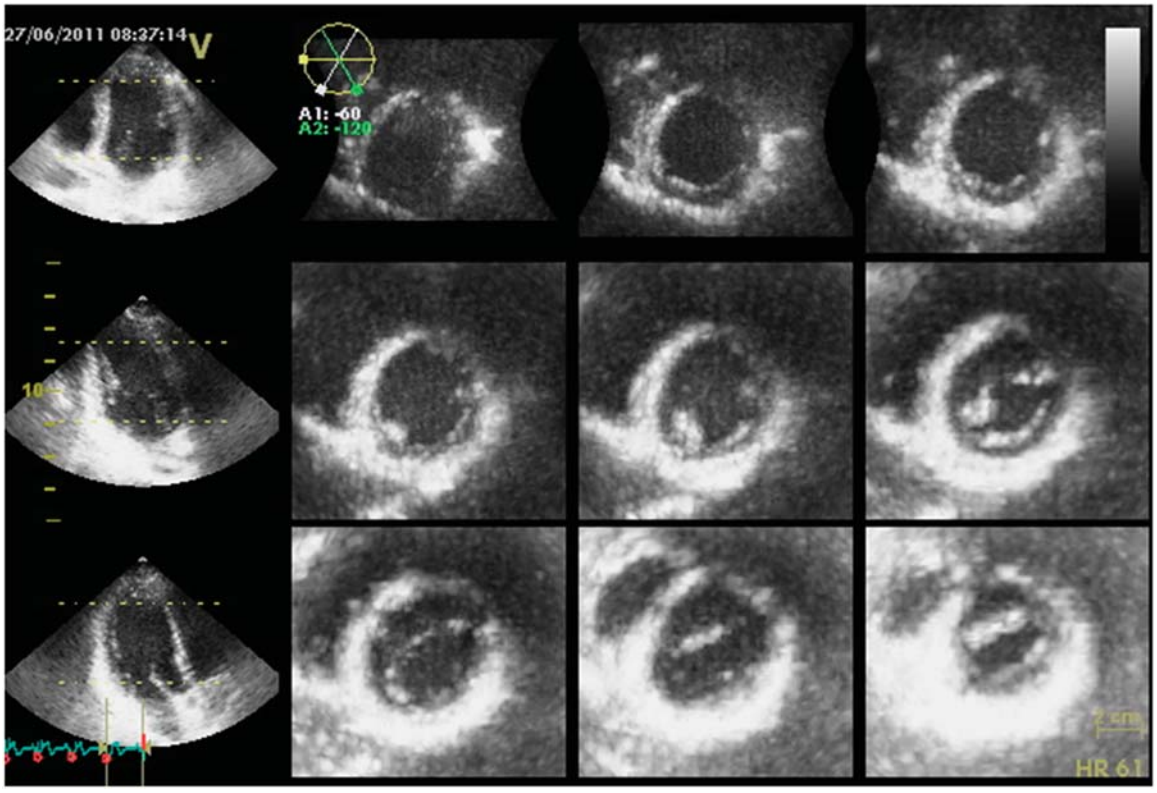

Figure 1 Twelve slice display of full-volume acuisition: nine short axis views (three basal, three middle, and three apical of the left ventricle) and three apical views (four-chamber, two-chamber and long-axis). By selecting 12-slice display mode available on the machine, the operator can be sure the entire left ventricular cavity and wall are included in the full volume before storing the volume data set.

using automated border detection with optional manual adjustment. RT3DE-derived LV mass was indexed for height powered to 2.7.[1]

3D strain is a post-processing tool that tracks 'speckles' in a 3D image from frame to frame in any of the three dimensions over time. By this software, the borders defined in the LV mass stage are propagated to end-systole, using the conservation of mass as a restriction, and used to define a region of interest (ROI) encompassing the LV myocardial wall. All areas inside the ROI (i.e. from the endocardium to the epicardium) are tracked. The quality of each match is automatically calculated and detected outliers are removed before obtaining weighted spatial averaging of the results. From the tracking results regional and global directional strains (longitudinal, circumferential, and radial) as well as the area strain can be generated and presented as strain curves and a colour-coded 17-segment bull's eye plot (*Figure 3*). Contrary to directional strains, which are calculated from changes of distance in their respective directions, the area strain (AS) is a measure of the relative % change in the area of a given myocardial segment, thus representing the percentage change of the myocardial surface from its original dimensions (*Figure 4*).[18]

AS is defined as

$$\mathrm{AS} = 100 \times \frac{(A - A_0)}{A_0},$$

where A is the instantaneous segmental area and A_0 is the end-diastolic area.

Radial strain (RS) is defined as

$$\mathrm{RS} = 100 \times \frac{(R - R_0)}{R_0},$$

where R and R_0 are the instantaneous and end-diastolic wall thickness, respectively. Assuming volume conservation, RS was estimated from the segmental areas as

$$\mathrm{RS} = 100 \times \frac{(A_0 - A)}{A}.$$

Global longitudinal strain (GLS), global circumferential strain (GCS), global area strain (GAS), and global radial strain (GRS) were calculated as weighted averages of the regional values from the 17 myocardial segments.

Using the software, two subsequent quality checks were performed during the analysis. The first tracking quality check is automatic: since the heart beats in a cyclic manner and the strain values are expected to be zero both at the start and end of the heart cycle, the algorithm automatically rejects myocardial segments that show a drift of more than 12% points. The second tracking quality check was performed by visual inspection of the tracking and myocardial segments and manual rejection of suboptimal tracking. The results of the rejected segments were then removed and excluded during calculation of global strain values. If more than three segments were rejected,

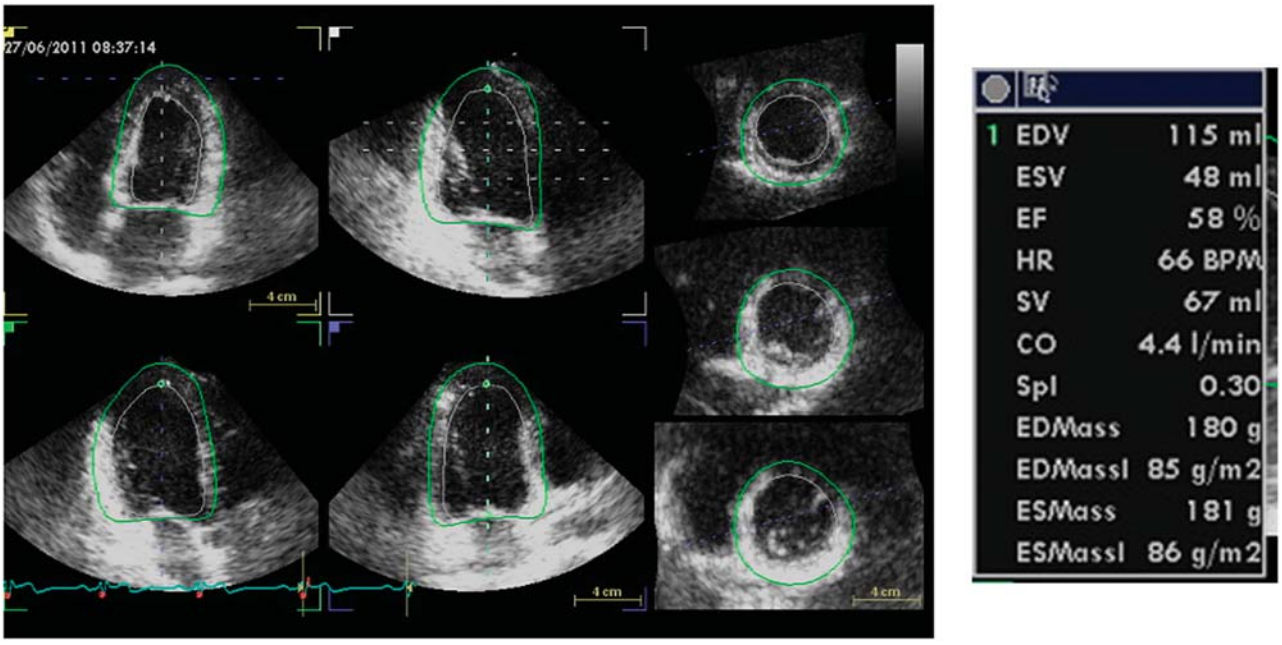

Figure 2 Automatic measurement of left ventricular function shape and mass by AutoLVQ software. The automatic tracing of the endocardial and epicardial border allows to obtain left ventricular end-diastolic and end-systolic volumes (EDV and ESV, respectively), ejection fraction (EF), stroke volume (SV), cardiac output (CO), sphericity index (SpI), and left ventricular mass [either at end-diastole (EDMass) or at end-systole (ESMass)].

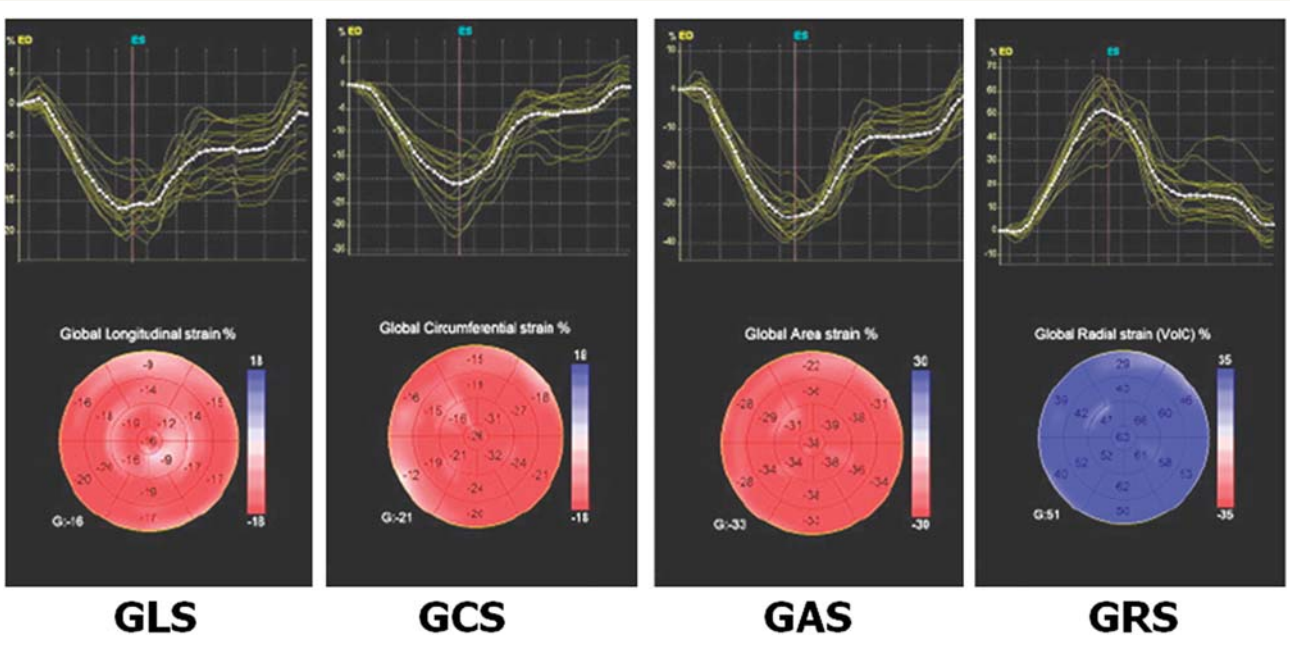

Figure 3 By using the novel advancement of AutoLVQ software, regional longitudinal, circumferential, and radial strain as well as area strain are generated and presented in both (regional and average) strain curves and colour- coded 17-segment bull's eye plot. Colour lines refer to regional strain; white dotted line is global (average) strain. Curves of longitudinal strain, circumferential strain, and area strain are negative (sign −), whereas curves of radial strain are positive (sign +). GAS, Global area strain; GCS, Global circumferential strain; GLS, Global longitudinal strain; GRS, Global radial strain.

global strain values were not calculated. In the present study, patients with ≥3 rejected segments were excluded from statistical analysis.

Statistical analyses

Statistical analysis was performed by SPSS package, release 12 (SPSS Inc, Chicago, IL, USA). Data are presented as mean values ± SD. Reproducibility analyses (intra- and inter-observer variability) were performed by calculating intra-class correlation coefficients (rho). Bland–Altman plot between inter-observer difference and average value was generated for GAS. Comparison between groups was obtained by one-factor analysis of variance and χ^2 distribution with computation of the exact *P*-value by the Monte-Carlo method. Least squares linear regression was used to evaluate univariate and multivariate correlates of a given variable. Multiple linear regression analyses were used to identify the independent correlates of 3D strain components. The null hypothesis was rejected at $P \leq 0.05$.

Results

Table 1 summarizes both intra- and inter-observer variability of the main RT3DE parameters in 25 subjects (15 normotensives and 10 hypertensives): the intra-class relation coefficients ranged between 0.803 and 0.917, thus showing excellent reproducibility. A Bland–Altman plot of the GAS inter-observer difference is depicted in *Figure 5*: the magnitude of agreement between the two observers is very good.

The characteristics of the study population are listed in *Table 2*. Age and HR were not significantly different between the two groups, whereas body mass index (BMI) and BP values were higher in hypertensive patients. Of note, nine hypertensive patients had a BMI >28 kg/m^2 and three >30 kg/m^2 (data not shown in the table).

Data of standard echo-Doppler examinations are reported in *Table 3*. Hypertensive patients had higher LV mass and relative wall thickness and significant changes of Doppler-derived diastolic parameters in comparison with healthy controls, without a difference of the EF. Clear-cut LV hypertrophy (LV mass/height$^{2.7}$ ≥45 g/m$^{2.7}$ in women and ≥49 g/m$^{2.7}$ in men)[1] was not found in any of the hypertensive patients (data not in the table).

RT3DE assessment of LV function is summarized in *Table 4*. The EDV, ESV, SV, CO, EF, and sphericity index did not differ significantly between the two groups. 3D LV mass and LV mass index (LVMi) were

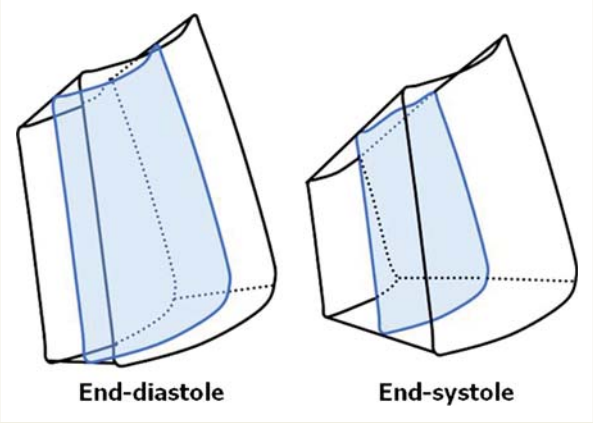

Figure 4 Schematic representation of the myocardial area strain depicted in azure colour. At end-diastole (left part) the myocardial surface area is represented in its unstressed original dimensions. During systole, the size of the surface area decreases because of deformation of the myocardial segment reaching its maximum at end-systole (right part).

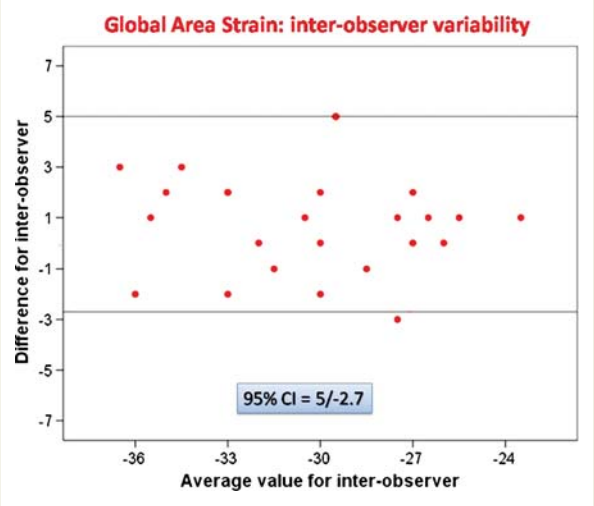

Figure 5 Bland–Altman plot of inter-observer difference of the global area strain. Continuous lines are 95% confidence intervals of between-measure differences.

Table 1 Reproducibility tests of the main three-dimensional parameters

Variable	Intra-observer variability, Rho (95% CI)	Inter-observer variability, Rho (95% CI)
EF	0.908 (0.805–0958), $P < 0.0001$	0.803 (0.438–0.922), $P < 0.0001$
LVM	0.917 (0.822–0.962), $P < 0.0001$	0.842 (0.658–0.929), $P < 0.0001$
GLS	0.906 (0.799–0.958), $P < 0.0001$	0.866 (0.719–0.939), $P < 0.0001$
GCS	0.889 (0.765–0.950), $P < 0.0001$	0.804 (0.604–0.909), $P < 0.0001$
GAS	0.904 (0.794–0.957), $P < 0.0001$	0.835 (0.647–0.925), $P < 0.0001$
GRS	0.899 (0.785–0.954), $P < 0.0001$	0.811 (0.621–0.912), $P < 0.0001$

Rho is the intra-class coefficient.
EF, Ejection fraction; GAS, Global area strain; CGS, Global circumferential strain; GLS, Global longitudinal strain; GRS, Global radial strain; LV mass.

Table 2 Demographics of the study population

Variable	Healthy controls ($n = 38$)	Hypertensives ($n = 38$)	*P*-value
Gender (M/F)	28/10	28/10	NS
Age (years)	29.7 ± 4.9 (20–39)	31.9 ± 6.9 (18–46)	NS
BMI (kg/m^2)	23.6 ± 2.4 (19–29)	27.4 ± 3.5 (22–41)	<0.0001
Systolic BP[a] (mmHg)	118.4 ± 8.5 (100–140)	143.7 ± 7.5 (130–160)	<0.0001
Diastolic BP[a] (mmHg)	73.6 ± 7.5 (60–85)	97.6 ± 4.6 (90–110)	<0.0001
Mean BP[a] (mmHg)	88.5 ± 7.6 (73–100)	113.0 ± 4.7 (103–127)	<0.0001
HR (bpm)	68.7 ± 11.0 (50–88)	70.7 ± 6.8 (54–82)	NS

Data expressed as mean ± SD (range in parenthesis).
BP, Blood pressure; BMI, Body mass index; HR, Heart rate.
[a]BP values as measured at the end of the echo examination.

Table 3 Standard echo-Doppler assessment

Variable	Healthy controls	Hypertensives	*P*-value
LV mass	145.7 ± 21.6	169.7 ± 22.9	<0.0001
LV mass index (g/m$^{2.7}$)	32.8 ± 4.1	39.4 ± 5.4	<0.0001
Relative wall thickness	0.30 ± 0.05	0.36 ± 0.06	<0.0001
EF (%)	56.3 ± 5.8	55.3 ± 4.4	NS
E/*A* ratio	1.58 ± 0.54	1.30 ± 0.41	<0.01
Deceleration time (ms)	176.3 ± 18.2	194.1 ± 33.9	<0.005
LAVi (mL/m^2)	25.6 ± 6.3	28.5 ± 3.8	<0.01
e′ velocity (cm/s)	13.9 ± 2.0	10.5 ± 2.3	<0.0001
E/e′ ratio	5.98 ± 8.6	7.21 ± 1.5	<0.0001

Data expressed as mean ± SD.
A, Transmitral *A* velocity; *E*, Transmitral *E* velocity; e′, e′ velocity of mitral annulus; EF, Ejection fraction; LAVi, Left atrial volume index; LV, Left ventricular.

Table 4 Real-time three-dimensional standard echocardiographic assessment

Variable	Healthy controls	Hypertensives	*P*-value
LV EDV (mL)	122.4 ± 27.9	132.5 ± 25.1	NS
LV ESV (mL)	51.6 ± 16.1	57.2 ± 16.1	NS
SV (mL)	70.8 ± 14.6	75.3 ± 13.8	NS
CO (L/m)	4.8 ± 1.0	5.2 ± 1.2	NS
LV EF (%)	58.5 ± 5.9	57.5 ± 6.1	NS
Sphericity index	0.40 ± 0.13	0.41 ± 0.10	NS
LV mass	128.4 ± 17.0	146.9 ± 15.9	<0.0001
LV mass index (g/m$^{2.7}$)	28.7 ± 3.3	34.1 ± 4.1	<0.0001
GLS (%)	−20.9 ± 2.7	−18.3 ± 2.1	<0.0001
GCS (%)	−17.4 ± 2.2	−16.8 ± 2.0	NS
GAS (%)	−33.6 ± 3.4	−29.1 ± 2.5	<0.0001
GRS (%)	53.6 ± 7.6	47.0 ± 6.8	<0.0001

Data expressed as mean ± SD.
CO, Cardiac output; EDV, End-diastolic volume; EF, Ejection fraction; ESV, End-systolic volume; GAS, Global area strain; GCS, Global circumferential strain; GLS, Global longitudinal strain; GRS, Global radial strain; LV, Left ventricular; SV, Stroke volume.

greater in hypertensive patients than in healthy controls (all $P < 0.0001$). LV mass was significantly lower by RT3DE than by M-mode (-20.6 ± 13.5 g, $P < 0.0001$) (data not in the table). GLS, GAS, and GRS (all $P < 0.0001$) were significantly reduced in hypertensive patients, while GCS was similar between the two groups.

Table 5 summarizes the univariate relations of 3D-derived strain in the pooled population. Among the strain components GAS showed the strongest associations with BP and RT3DE-derived LV mass. *Figure 6* displays the scatterplot between GAS and both mean BP and LVMi.

The results of separate multivariable regression analyses performed to test the independent relation of 3D strain components in the pooled population are reported in *Table 6*. Among the different 3D strain components, GAS showed the best independent associations with mean BP ($\beta = -0.502$, $P < 0.0001$) and LVMi ($\beta = -0.385$, $P < 0.001$).

Discussion

The present study examined LV structure and systolic function in newly diagnosed hypertensive patients by an RT3DE assessment of LV volumes, mass, and strain components. To the best of our knowledge, this is the first study to use this quantitative approach as an alternative to standard echocardiography in native arterial hypertension. This new approach confirms the increase of the LV mass detectable also by standard echocardiography but allows an additional, reliable detection of early myocardial deformation abnormalities. It is worthy of note that these abnormalities involved GLS, GRS, and GAS and were evident in patients without LV hypertrophy and with only minor changes of the LV geometry and normal EF. All the parameters obtained by RT3DE had very good reproducibility and therefore appear sufficiently reliable to be used in the setting of hypertensive patients.

In current clinical practice standard 2D echocardiography is the elective tool to diagnose changes of the LV geometry, corresponding to LV concentric remodelling and concentric or eccentric hypertrophy in uncomplicated arterial hypertension.[19] RT3DE

Table 5 Univariate relations (*r* coefficient and significance) of three-dimensional-derived strain components in the pooled population[a]

Variable	GLS (*P*-value)	GCS (*P*-value)	GAS (*P*-value)	GRS (*P*-value)
BMI	−0.31 (<0.005)	−0.24 (<0.05)	−0.41 (<0.0001)	−0.34 (<0.005)
Systolic BP	−0.40 (<0.0001)	−0.29 (<0.01)	−0.60 (<0.0001)	−0.48 (<0.0001)
Diastolic BP	−0.39 (<0.0001)	−0.30 (<0.01)	−0.56 (<0.0001)	−0.49 (<0.0001)
Mean BP	−0.41 (<0.0001)	−0.30 (<0.01)	−0.59 (<0.0001)	−0.50 (<0.0001)
3D EF	0.35 (<0.002)	0.47 (<0.0001)	0.45 (<0.0001)	0.47 (<0.0001)
3D LV mass	−0.49 (<0.0001)	−0.26 (<0.05)	−0.51 (<0.0001)	−0.48 (<0.0001)
3D LV mass index	−0.46 (<0.001)	−0.25 (<0.05)	−0.49(<0.0001)	−0.39 (<0.001)
E/*A* ratio	0.23 (<0.05)	0.15 (NS)	0.36 (<0.002)	0.26 (<0.02)
e′ velocity	0.58 (<0.0001)	0.22 (<0.05)	0.57 (<0.0001)	0.49 (<0.0001)
E/e′ ratio	−0.46 (<0.0001)	−0.22 (<0.05)	−0.38 (<0.001)	−0.33 (<0.005)

Abbreviations as in *Tables 2*, *3*, and *4*.
[a]Values of GLS, GCS, and GAS considered as 'positive' (sign +) to build the univariate relations in order to homogenize the results of analyses and strengthen their clinical meaning: the higher the values, the better is the strain deformation independent of the plus/minus sign.

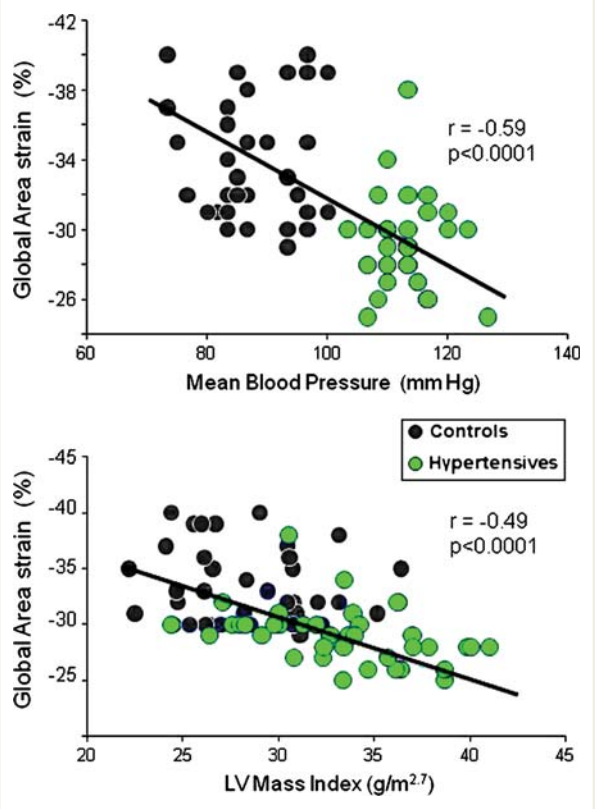

Figure 6 Scatterplot and regression lines of individual values of the global area strain (*x*-line) and corresponding values of both mean blood pressure (top of the figure) and LV mass index (bottom) (*y*-line) in healthy controls and hypertensive patients. LV, Left ventricular.

Table 6 Independent correlates of three-dimensional-derived strain components in the pooled population[a]

Dependent variable	Covariate	B Coefficient	*P*-value
GLS[b]	BMI	−0.101	NS
	Mean BP	−0.132	NS
	LVMi	−0.264	<0.01
	EF	0.249	<0.01
	E/e′ ratio	−0.242	<0.02
GCS[c]	BMI	−0.091	NS
	Mean BP	−0.377	<0.01
	LVMi	−0.162	NS
	EF	0.534	<0.0001
	E/e′ ratio	−0.07	NS
GAS[d]	BMI	−0.068	NS
	Mean BP	−0.502	<0.0001
	LVMi	−0.385	<0.001
	EF	0.268	<0.01
	E/e′ ratio	−0.11	NS
GRS[e]	BMI	−0.120	NS
	Mean BP	−0.470	<0.0001
	LVMi	−0.261	<0.01
	EF	0.543	<0.0001
	E/e′ ratio	−0.08	NS

SEE, standard error estimated. Other abbreviations as in *Tables 2* and *4*.
[a]Values of GLS, GCS, and GAS considered as 'positive' (sign +) to build the associations in order to homogenize the results of analyses and strengthen their clinical meaning: the higher the values, the better is the strain deformation independent of the plus/minus sign.
[b]Cumulative $R^2 = 0.34$, SEE = 2.28%, $P < 0.0001$.
[c]Cumulative $R^2 = 0.33$, SEE = 1.72%, $P < 0.0001$.
[d]Cumulative $R^2 = 0.55$, SEE = 2.71%, $P < 0.0001$.
[e]Cumulative $R^2 = 0.52$, SEE = 5.62%, $P < 0.0001$.

can easily provide additional insights. Several studies have successfully compared RT3DE with cardiac magnetic resonance for the assessment of the LV mass in multiple clinical settings.[20–28] Our findings extend these results demonstrating the ability of RT3DE in detecting even a mild increase of the LV mass in new-onset arterial hypertension where the patients are too young to

produce evidence of clear-cut LV hypertrophy. It is noteworthy that RT3DE estimation of the LV mass is very advantageous since it does not depend on any geometric assumption of the left ventricle and is relatively operator-independent owing to its semi-automatic approach.[29]

The assessment of the different components of myocardial deformation in hypertensive patients has been performed recently by using 2D STE. Longitudinal strain was found to be reduced when the EF and both radial and circumferential strain are still normal.[8] These changes become even more evident in the presence of LV hypertrophy.[9] The alteration of hypertensive longitudinal strain is reported to be associated with LV diastolic abnormalities,[8] as a possible consequence of alteration in collagen turnover and development of myocardial fibrosis.[10]

Compared with 2D STE, RT3DE-derived STE presents a number of advantages. Detection by 2D STE on a single tomographic plane is impaired by out-of-plane motion, while RT3DE-derived STE can track motion of the speckles irrespective of their direction, as long as they remain within the selected scan volume,[7] an aspect that might be particularly relevant in the quantification of radial strain.

While the early impairment of 3D GLS and the preservation of GCS in the early stages of hypertensive heart disease are consistent with previous findings obtained by 2D STE,[8] the reduction of 3D GRS is discordant with 2D STE findings.[8,9] This discrepancy is attributable to the substantial approximation in the assessment of 2D GRS. By using the 2D approach, GRS is less robust and reproducible than GLS and GCS,[30,31] because of the need to evaluate multiple levels (basal, mid, and apical short-axis view) in different heart beating, and the different impact of the undetectable third displacement vector.[32] In contrast, RT3DE-derived STE does not have the limitation of being calculated on arbitrary slices,[7] which could lead to the very acceptable reproducibility of GRS measurements showed in the present study. However, further studies are needed to confirm this finding in larger sample sizes of hypertensive cohorts.

Another important and new finding of the present study is represented by the evidence of impaired GAS in our young native hypertensive patients. GAS is a new 3D STE index which corresponds to the percentage change of the myocardium from its original dimensions[18] and allows a relatively operator-independent quantitative evaluation of global and regional LV function. The regional area strain has been demonstrated to have the capability of exploring regional wall motion abnormalities more accurately than visual assessment.[33] GAS correlates very well with both EF and wall motion score index,[34] identifies mechanical dyssynchrony,[13] and responds to cardiac resynchronization therapy.[35] In the present study GAS confirmed a good association with EF but was also the strain component to show the most significant independent association with the degree of BP and the magnitude of LVMi. GAS appears therefore as a comprehensive functional parameter that is influenced by both afterload and LV mass, i.e. two major recognized factors affecting a hypertensive heart. Of note, a stronger negative association between LV mass and GAS could not be expected in the present population, which included native young hypertensive patients without clear-cut LV hypertrophy.

Limitations

Despite the operator-independency in reading performance, RT3DE assessment of LV structure and function can be influenced by the quality of basic ultrasound imaging and requires some technical skills in order to encompass the whole of the LV cavity and wall while maintaining an adequate frame rate during the full-volume acquisition. The feasibility of RT3DE in the present study was very high in both the pooled population (8 exclusions on originally 84 screened patients: 90.5% feasibility) and in the hypertensive setting (5 exclusions on 43: 88.4% feasibility) of the present study. However, the recruited patients were young and none had clear-cut LV hypertrophy. This approach could become more difficult in hypertrophic hearts and has therefore to be verified in patients with a higher degree of LV mass.

Another limitation corresponds to the lack in comparison of 3D strain data derived from the equipment and software we used with different echocardiographic machines with similar capabilities (inter-vendor or machine-to-machine variability). 3D STE-derived LV deformation parameters have been recently demonstrated to be highly vendor dependent.[36] This is a relevant issue because reasonable levels of reproducibility and vendor independence are crucial requirements for this methodology to become unquestionably useful in the clinical setting.

Perspectives

A novel approach by real-time 3D echocardiography—as we show in the present study—can be useful to characterize the features of early functional abnormalities and their determinants in the hypertensive heart. The global area strain is a comprehensive parameter of myocardial systolic deformation and is very sensitive to both changes of afterload and LV mass. Further studies are needed to characterize mechanically this new index of LV function and to verify whether the reported modifications can be offset by antihypertensive therapy.

Acknowledgements

We acknowledge Luigi Badano and Denisa Muraru for their precious teaching of RT3DE.

Conflict of interest: none declared.

References

1. Lang RM, Bierig M, Devereux RB, Flachskampf FA, Foster E, Pellikka PA *et al.* Chamber quantification working group; American Society of Echocardiography's Nomenclature and Standards Committee; European Association of Echocardiography. Recommendations for chamber quantification: a report from the American Society of Echocardiography's Guidelines and Standard Committee and the Chamber Quantification Writing Group, developed in conjunction with the European Association of Echocardiography. *Eur J Echocardiogr* 2006;**7**:79–108.
2. Levy D, Garrison RJ, Savage DD, Kannel WB, Castelli WP. Prognostic implications of echocardiographically determined left ventricular mass in the Framingham Heart Study. *N Engl J Med* 1990;**322**:1561–6.
3. Devereux RB, Wachtell K, Gerdts E, Boman K, Nieminen MS, Papademetriou V *et al.* Prognostic significance of left ventricular mass change during treatment of hypertension. *J Am Med Assoc* 2004;**292**:2350–6.
4. Klingbeil AU, Schneider M, Martus P, Messerli FH, Schmieder RE. A meta-analysis of the effects of treatment on left ventricular mass in essential hypertension. *Am J Med* 2003;**115**:41–6.
5. de Simone G, Devereux RB, Roman MJ, Ganau A, Saba PS, Alderman MH *et al.* Assessment of left ventricular function by the midwall fractional shortening/end-systolic stress relation in human hypertension. *J Am Coll Cardiol* 1994;**23**:1444–51.

6. Galderisi M. Diagnosis and management of left ventricular diastolic dysfunction in the hypertensive patients. *Am J Hypertens* 2011;**24**:507–17.
7. Mor-Avi V, Lang RM, Badano LP, Belohlavek M, Cardim NM, Derumeaux G *et al.* Current and evolving echocardiographic techniques for the quantitative evaluation of cardiac mechanics: ASE/EAE consensus statement on methodology and indications endorsed by the Japanese Society of Echocardiography. *Eur J Echocardiogr* 2011;**12**:167–205.
8. Galderisi M, Lomoriello VS, Santoro A, Esposito R, Olibet M, Raia R *et al.* Differences of myocardial systolic deformation and correlates of diastolic function in competitive rowers and young hypertensives: a speckle-tracking echocardiography study. J Am Soc Echocardiogr 2010;**23**:1190–1198.
9. Kouzu H, Yuda S, Muranaka A, Doi T, Yamamoto H, Shimoshige S *et al.* Left ventricular hypertrophy causes different changes in longitudinal, radial and circumferential mechanics in patients with hypertension: a two-dimensional Speckle Tracking study. *J Am Soc Echocardiogr* 2011;**24**:192–9.
10. Kang SJ, Lim HS, Choi B, Choi SY, Yoon MH, Hwang GS *et al.* Longitudinal strain and torsion assessed by two-dimensional speckle tracking correlate with the serum level of tissue inhibitor of matrix metalloproteinase-1, a marker of myocardial fibrosis, in patients with hypertension. *J Am Soc Echocardiogr* 2008;**21**:907–11.
11. De Isla LP, Balcones DV, Fernandez-Golfin C, Marcos-Alberca P, Almeria C, Rodrigo JL. Three-dimensional wall motion tracking: a new and faster tool for myocardial strain assessment: comparison with two-dimensional wall motion tracking. *J Am Soc Echocardiogr* 2009;**22**:325–30.
12. Maffesanti F, Nesser HJ, Weinert L, Steringer-Mascherbauer R, Niel J, Gorissen W *et al.* Quantitative evaluation of regional left ventricular function using three-dimensional speckle tracking echocardiography in patients with and without heart disease. *Am J Cardiol* 2009;**104**:1755–62.
13. Thebault C, Donal E, Bernard A, Moreau O, Schnell F, Mabo P *et al.* Real-time three-dimensional speckle tracking echocardiography: a novel technique to quantify global left ventricular mechanical dyssynchrony. *Eur J Echocardiogr* 2011;**12**:26–32.
14. Mancia G, De Backer G, Dominiczak A, Cifkova R, Fagard R, Germano G *et al.* for ESH-ESC task force on the management of arterial hypertension: 2007 ESH-ESC practice guidelines for the management of arterial hypertension: ESH-ESC task force on the management of arterial hypertension. *J Hypertens* 2007;**25**:1105–87.
15. Innelli P, Sanchez R, Olibet M, Esposito R, Galderisi M. The impact of age on left ventricular longitudinal function in healthy subjects: a pulsed Tissue Doppler study. *Eur J Echocardiogr* 2008;**9**:241–9.
16. Nagueh SF, Appleton CP, Gillebert TC, Marino PN, Oh JK, Smiseth OA *et al.* Recommendations for the evaluation of left ventricular diastolic function by echocardiography. *Eur J Echocardiogr* 2009;**10**:165–93.
17. Muraru D, Badano LP, Piccolo G, Gianfagna P, Del Mestre L, Ermacora D *et al.* Validation of a novel automated border detection algorithm for rapid and accurate quantitation of left ventricular volumes based on three-dimensional echocardiography. *Eur J Echocardiogr* 2010;**2**:359–68.
18. Langeland S, Rabben SI, Heimdal A, Gérard O. 4D Strain: validation of new 3D speckle tracking and left ventricular tool in simulated echocardiographic data. *Eur J Echocardiogr* 2010;**11**(suppl 2):Abstract P658.
19. Agabiti-Rosei E, de Simone G, Mureddu GF, Trimarco B, Verdecchia P, Volpe M. Arterial Hypertension and Cardiac Damage: Diagnostic and Therapeutic Guidelines. *High Blood Press Cardiovasc Prev* 2008;**15**:141–69.
20. Jenkins C, Bricknell K, Hanekom L, Marwick TH. Reproducibility and accuracy of echocardiographic measurements of left ventricular parameters using real-time three-dimensional echocardiography. *J Am Coll Cardiol* 2004;**44**:878–86.
21. Bicudo LS, Tsutsui JM, Shiozaki A, Rochitte CE, Arteaga E, Mady C *et al.* Value of real-time three-dimensional echocardiography in patients with hypertrophic cardiomyopathy: comparison with two-dimensional echocardiography and magnetic resonance imaging. *Echocardiography* 2008;**25**:717–26.
22. Mor Avi V, Sugeng L, Weinert L, MacEneaney P, Caiani EG, Koch R *et al.* Fast measurement of left ventricular mass with real-time three-dimensional echocardiography: comparison with magnetic resonance imaging. *Circulation* 2004;**110**:1814–8.
23. Caiani EG, Corsi C, Sugeng L, MacEneaney P, Weinert L, Mor-Avi V *et al.* Improved quantification of left ventricular mass based on endocardial and epicardial surface detection with real time three dimensional echocardiography. *Heart* 2006;**92**:213–9.
24. Oe H, Hozumi T, Arai K, Matsumura Y, Negishi K, Sugioka K *et al.* Comparison of accurate measurement of left ventricular mass in patients with hypertrophied hearts by real-time three-dimensional echocardiography versus magnetic resonance imaging. *Am J Cardiol* 2005;**95**:1263–7.
25. Van den Bosch AE, Robbers-Visser D, Krenning BJ, McGhie JS, Helbing WA, Meijboom FJ *et al.* Comparison of real-time three-dimensional echocardiography to magnetic resonance imaging for assessment of left ventricular mass. *Am J Cardiol* 2006;**97**:113–7.
26. Qin JX, Shiota T, Thomas JD. Determination of left ventricular volume, ejection fraction, and myocardial mass by real-time three-dimensional echocardiography. *Echocardiography* 2000;**17**:781–986.
27. Yap SC, van Geuns RJ, Nemes A, Meijboom FJ, McGhie JS, Geleijnse ML *et al.* Rapid and accurate measurement of LV mass by biplane real-time 3D echocardiography in patients with concentric LV hypertrophy: comparison to CMR. *Eur J Echocardiogr* 2008;**9**:255–60.
28. Takeuchi M, Nishikage T, Mor-Avi V, Sugeng L, Weinert L, Nakai H *et al.* Age- and gender-dependency of left ventricular geometry assessed with real-time three-dimensional transthoracic echocardiography. *J Am Soc Echocardiogr* 2008;**21**:1001–5.
29. Mor Avi V, Lang RM. The use of real-time three-dimensional echocardiography for the quantification of left ventricular volumes and function. *Curr Opin Cardiol* 2009;**24**:402–9.
30. Donal E, Bergerot C, Thibault H, Ernande L, Loufoua J, Augeul L *et al.* Influence of afterload on left ventricular radial and longitudinal systolic functions: a two-dimensional strain imaging study. *Eur J Echocardiogr* 2009;**10**:914–21.
31. Marwick TH. Consistency of myocardial deformation imaging between vendors. *Eur J Echocardiogr* 2010;**11**:414–6.
32. Mavinkurve-Groothuis AM, Weijers G, Groot-Loonen J, Pourier M, Feuth T, de Korte CL *et al.* Interobserver, intraobserver and intrapatient reliability scores of myocardial strain imaging with 2-d echocardiography in patients treated with anthracyclines. *Ultrasound Med Biol* 2009;**35**:697–704.
33. Saito K, Okura H, Watanabe N, Hayashida A, Obase K, Imai K *et al.* Comprehensive evaluation of left ventricular strain using speckle tracking echocardiography in normal adults: comparison of three-dimensional and two-dimensional approaches. *J Am Soc Echocardiogr* 2009;**22**:1025–30.
34. Klejin SA, Aly MFA, Terwee CB, van Rossum AC, Kamp O. Three-dimensional Speckle Tracking Echocardiography for automatic assessment of global and regional left ventricular function based on area strain. *J Am Soc Echocardiogr* 2011;**24**:314–21.
35. Tatsumi K, Tanaka H, Tsuji T, Kaneko A, Ryo K, Yamawaki K *et al.* Strain dyssynchrony index by three-dimensional speckle area tracking can predict respond to cardiac resynchronization therapy. *Cardiovasc Ultrasound* 2011;**9**:11.
36. Gayat E, Ahmad H, Weinert L, Lang RM, Mor Avi V. Reproducibility and inter-vendor variability of left ventricular deformation measurements by three-dimensional Speckle Tracking echocardiography. *J Am Soc Echocardiogr* 2011;**24**:878–85.